

RESEARCH

Open Access



Added value of a chest multidetector computed tomography scoring system in the assessment of chronic lung disease among pediatric patients

Mona Ahmed Fouad Hafez^{1*} , Chandan Kumar Singh¹, Yasmin Saied Aly Sayed² and Reham Osama Mahmoud¹

Abstract

Background: Pediatric chronic lung disease (CLD) represents a heterogeneous group of several distinct clinical entities, with its prevalence increasing over the last decade. The current study aimed to identify the role of chest multidetector computed tomography (MDCT) using modified Bhalla scoring for the early diagnosis of CLD in pediatric patients and determine the most common chest MDCT findings. This prospective study involved 45 pediatric patients with chronic respiratory symptoms, all of whom underwent MDCT. Thereafter, data were analyzed using the modified Bhalla score.

Results: Chronic lung diseases were classified according to their radiological and clinical criteria. The total CT score, which was the most significant factor for chronic inhalation and chronic recurrent inflammatory lung diseases, varied between 2 and 21 points, with those having autoimmune diseases exhibiting the largest value for the mean CT score. The clinical severity of symptoms was not correlated with CT score.

Conclusion: Our findings showed that MDCT was a useful tool for diagnosing pediatric CLD and assessing disease extent, severity, and superimposed complications. The modified Bhalla CT scoring system allowed for systematic primary and follow-up assessments of various lung lesions in cases with varying CLD etiologies.

Keywords: Computed tomography, Multidetector, Pediatric chest, Chronic lung disease

Background

Pediatric chronic lung disease (CLD) represents a heterogeneous group of several distinct clinical entities. The prevalence of CLD has increased over the last decade due to more advanced and intensive respiratory support provided to at-risk infants, as well as the overall improvement in the survival of premature infants. The most common causes of CLD in children include cystic

fibrosis (CF), with other causes including bronchiectasis (e.g., immunodeficiency in third-world countries and postinfectious bronchiectasis, for instance after measles), bronchopulmonary dysplasia (BPD), chronic gastroesophageal reflux disease, aspiration pneumonitis, obstructive bronchiolitis disease, and childhood interstitial lung disease (chILD) [1, 2].

With the advances in multidetector computed tomography (MDCT), it is now possible to image the lung for ≤ 10 s and visualize the bronchial tree, lobes, and airways from the fifth -to the seventh-generation bronchi, as well as lung regions. This allows the accurate characterization of attributes, such as density, texture, aeration, and

*Correspondence: mona.fouad@kasralainy.edu.eg

¹ Diagnostic Radiology and Intervention, Kasr-Alainy Hospital, Cairo University Medical School, Cairo, Egypt
Full list of author information is available at the end of the article

distribution of the lungs [3]. MDCT can cover large volumes during simple breath-holding, with good longitudinal, intrinsic spatial resolution and temporal resolution. The results obtained from the dataset allow the generation of enhanced multi-surface and three-dimensional images of the airway, including those obtained from techniques developed specifically for airway imaging, such as virtual bronchography and virtual bronchoscopy [4]. CT can reveal lung damage, such as bronchial wall thickening, bronchiectasis, mucus obstruction, and areas of consolidation or atelectasis of the lung, which are difficult to detect using a pulmonary function test (PFT). Recent studies in children with CF have shown that structural damage visible on MDCT precedes changes revealed via PFT [5].

Since 1991, several chest MDCT scoring systems have been developed to observe the extent and severity of CF. This system had originally been introduced by Bhalla et al. and has since been modified by several authors [6, 7]. The images are scored using a modified Bhalla scoring system, which includes an evaluation of acinar nodules, interlobular septa thickening, ground glass and mosaic perfusion on inspiratory images, and air trapping on expiratory images. These changes are commonly observed and included in present scoring systems for CF lung disease. The total score is then derived by adding the scores for each abnormality and can range from 0 to 37 [8].

The current study aimed to identify the role of chest MDCT using a modified Bhalla scoring for the early diagnosis of CLD in pediatric patients and determine the most common chest MDCT findings and their correlation with clinical severity.

Methods

This prospective cohort study involved 45 patients referred from the Department of Pediatrics who underwent CT of the chest at the radiology department. The planned study duration was 6 months. This study was conducted according to the guidelines of the Ethical Committee and was approved by its institutional review board.

The inclusion criteria were pediatric patients who had a history of chronic respiratory symptoms throughout a period of 6 months, from January 2021 to June 2021; all cases with an acceptable quality of current chest CT; and those diagnosed with chronic lung injury after following up on previous diagnostic test. The exclusion criteria were patients with the chronic respiratory disorder who were unable to hold their breath during MDCT scanning.

Patients were clinically assessed at the pediatric chest clinic where they underwent comprehensive history taking, clinical examination, and relevant laboratory

examinations (e.g., complete blood count, C-reactive protein, sputum culture). MDCT of the chest was performed using a GE Brightspeed Elite 16 MDCT scanner, with the following parameters: helical scan; 100 kV; 199 mA; field of view, 320 mm from the root of the neck to level of the renal arteries; slice thickness, 1.25 mm; slice interval, 5 mm. The total exposure time was 16 s, with a matrix size of 512×512 .

Patients were positioned supine, with fixed inspiration and arms extended overhead. The area from the top of lungs through the bottom of lungs was scanned while instructing cooperative patients to hold their breath at inspiration. However, for uncooperative children, quiet respiration was determined after administering a light universally approved sedative, such as chloral hydrate.

All volumetric chest CT images were assessed at a lung window of WW 1500, WL 500 and a mediastinal window of WW 400, WL 40.

Data analysis

Two radiologists, both having 16 years of experience in chest and pediatric imaging, reviewed all the chest MDCT images separately along with the clinical data, laboratory data, and previous radiology reports. The location of the lesions was assessed for each chest CT. Chest CT assessment was based on the Bhalla scoring system described by Judge et al. [8] (Table 1), which evaluates the severity of bronchiectasis, peribronchial thickening, extent of bronchiectasis (number of pulmonary segments), the extent of mucus plugging, sacculations or abscesses, generation of bronchial divisions involved, number of bullae, emphysema, and collapse/consolidation. The total score for each item ranged from 0 to 3 except for emphysema, consolidation/collapse, mosaic attenuation, air trapping, and acinar nodules, which have a total score ranging from 0 to 2. All scores for each patient were then added in order to obtain the overall Bhalla score, which ranged up to 40.

Etiological diagnoses were classified as bronchopulmonary dysplasia (none throughout this study), inhalation lung disease (e.g., hypersensitivity pneumonitis, toxin inhalation), chronic recurrent inflammatory disease (e.g., recurrent viral/bacterial/fungal disease secondary to chronic disease, granulomatous, and aspiration), autoimmune disease, chronic airway disease (including suppurative lung syndrome and asthma), ILD (e.g., neuroendocrine hyperplasia of infancy, idiopathic pulmonary hemorrhage, usual interstitial pneumonia, Langerhans cell histiocytosis, and edema), hereditary malformations (e.g., congenital lobar emphysema, CF, and ciliary dyskinesia), and vascular disease (e.g., post-infarction).

Table 1 Modified Bhalla CT scoring system, described by Judge et al. [8]

CT abnormalities	CT score			
	0	1	2	3
Severity of bronchiectasis	Absent	Lumen slightly greater than adjacent vessel	Lumen 2–3 times adjacent vessel	Lumen more than 3 times adjacent vessel
Peribronchial thickening	Absent	Thickness equals adjacent vessel	Thickness less than 2 times adjacent vessel	Thickness more than 2 times adjacent vessel
Extent of bronchiectasis	Absent	1–5 BPS	6–9 BPS	More than 9 BPS
Generation of bronchial division	Absent	Up to 4th generation	Up to 5th generation	Up to 6th generation
Extent of mucus plugging	Absent	1–5 BPS	6–9 BPS	More than 9 BPS
Emphysema	Absent	1–5 BPS	More than 5 BPS	
Bullae	Absent	Unilateral	Bilateral	
Sacculation/abscesses	Absent	1–5 BPS	6–9 BPS	More than 9 BPS
Collapse/consolidation	Absent	Subsegmental	Segmental/lobar	
Mosaic perfusion	Absent	1–5 BPS	More than 5 BPS	
Air trapping	Absent	1–5 BPS	More than 5 BPS	
Acinar nodules	Absent	Subsegmental/segmental	Lobar	Diffuse
Thickening of intralobular septation	Absent	Subsegmental/segmental	Lobar	Diffuse
Ground glass	Absent	Subsegmental/segmental	Lobar	Diffuse

BPS Bronchopulmonary segment

Statistical analysis

Data were coded and entered using the Statistical Package for the Social Sciences version 26 (IBM Corp., Armonk, NY, USA). Categorical data were expressed as numbers and percentages. Spearman's correlations were determined, with P values < 0.05 indicating statistical significance.

Results

Demographics

A total of 45 patients were included in our final analysis, among whom 34 (75.6%) and 11 were males and females (24.4%), respectively. The patients had a mean age of 7.17 ± 4.56 years (range, 1–18 years).

Bhalla CT score

The total CT score varied between 2 and 21 points among the included patients, with a mean score of 6.7 ± 4.66 . The largest proportion of patients (20%) had a score of 3, whereas 17.8%, 11.1%, and 11.1% had a score of 5, 2, and 4, respectively (Fig. 1).

Chronic lung disease distribution in the studied cases: correlation between disease extent and chest CT components of the Bhalla score

Bilateral disease was present in 75.6% of the cases. The most affected lung lobes were the lower zone (84.4%), followed by the upper zone (73.3%) (Fig. 2).

After determining the correlation between various chest CT findings and different etiological diagnosis, we found that the severity, extent, and generalities of bronchial division involvement of bronchiectasis were correlated with disease bilaterality ($P = 0.013$, 0.006 , and 0.007 , respectively). Moreover, the bilateral disease was significantly correlated with collapse/consolidation, which has been mainly noted in chronic recurrent infection ($P = 0.008$). Furthermore, the increase in the total CT score was positively correlated with disease bilaterality and negatively correlated with unilateral disease ($P = 0.004$ and 0.025 , respectively).

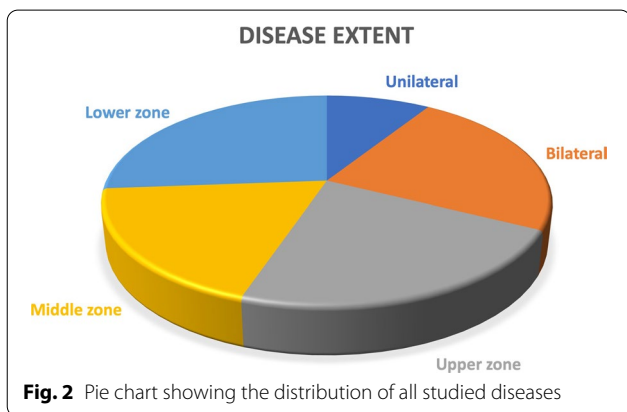
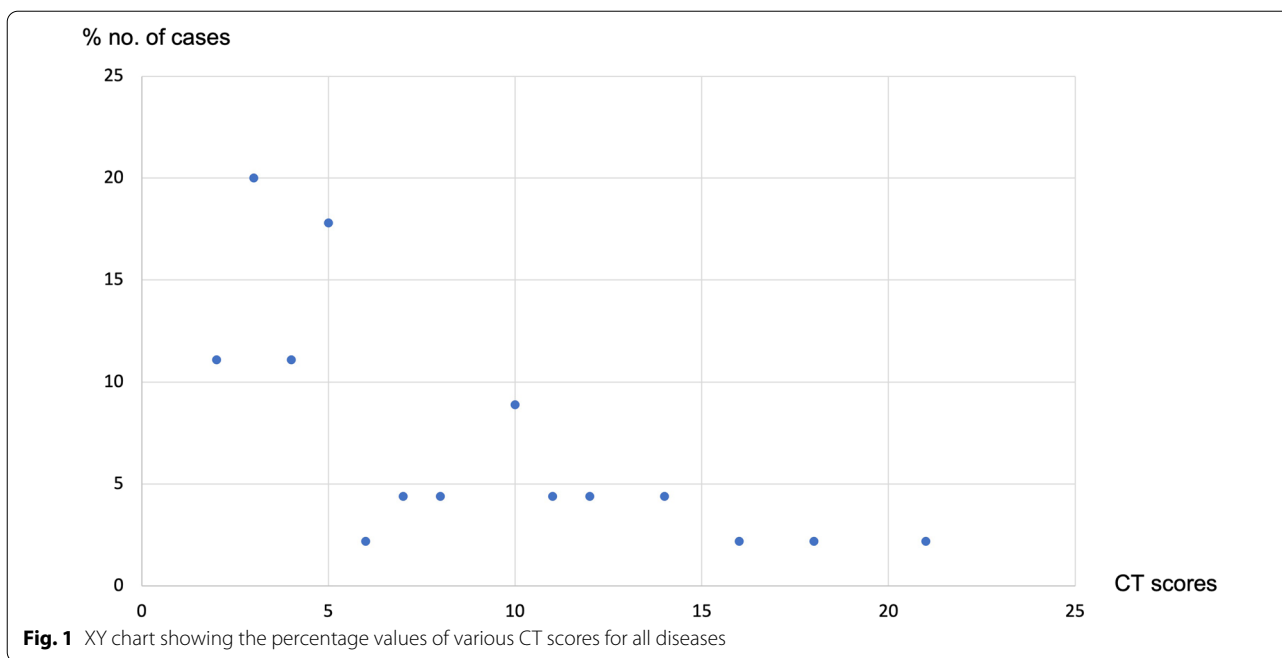
Acinar nodules were significantly correlated with upper and middle lung lobe localization ($P = 0.048$ and 0.003 , respectively).

Chest CT components of the modified Bhalla CT score

The most commonly encountered CT chest finding was mild peribronchial thickening (46.7%) and mild ground-glass opacities (44.4%), followed by mild bronchiectasis (33.3%) and segmental or lobar collapse (31.1%) (Fig. 3).

Etiology of chronic lung disease in the studied cases

The most commonly encountered chronic lung disease (CLD) was chronic recurrent inflammatory diseases (66.7%), which had the highest total CT score, followed by interstitial lung disease and chronic airway disease (20% for each). The sub-etiology for each etiological



diagnosis throughout the study duration is illustrated in Table 2. Associated etiologies encountered here included CF with chronic airway disease, infection with chronic airway disease, autoimmune disease with chronic inflammatory disease in a case, and ILD in another, as well as aspiration pneumonitis with sequestered lung. The calculated mean and total modified Bhalla CT score for various etiologies are displayed in Table 3, and the correlation for their significance is displayed in Table 4.

Correlation between etiological diagnosis and chest CT components of the Bhalla score

Inhalation lung disease was significantly correlated with mosaic attenuation, acinar nodules, and mean CT score

($P=0.023$, 0.004 , and 0.006 , respectively). Meanwhile, chronic recurrent inflammation was significantly correlated with collapse/consolidation, mosaic attenuation, and fibrosis/interlobular septal thickening ($P=0.01$, 0.008 , and 0.004) but was negatively correlated with mean CT score ($P=0.006$). Moreover, autoimmune disease was significantly correlated with the presence of air bubbles and emphysema ($P=0.001$ and 0.001 , respectively), while hereditary lung disease was significantly correlated with the severity of bronchiectasis and bronchial wall thickening ($P=0.007$ and 0.016 , respectively). Interstitial lung disease was significantly correlated with emphysema, fibrosis, and honeycombing ($P=0.044$, 0.00 , and 0.044 , respectively). Chronic airway disease was significantly correlated with air trapping ($P=0.026$), while chronic vascular disease was significantly correlated with abscess/sacculation ($P=0.001$).

Correlation between CT score and clinical severity

Among the included cases, seven had type I, II, and III respiratory distress, the CT scores of whom varied from 2 to 21, with a mean score of 7.5. One case had known cardiac disease.

Discussion

Noticeable confusion has existed regarding the nomenclature, classification, and management of pediatric diffuse lung diseases [9]. In this study, CLD was classified as inhalation lung disease, chronic recurrent inflammatory,

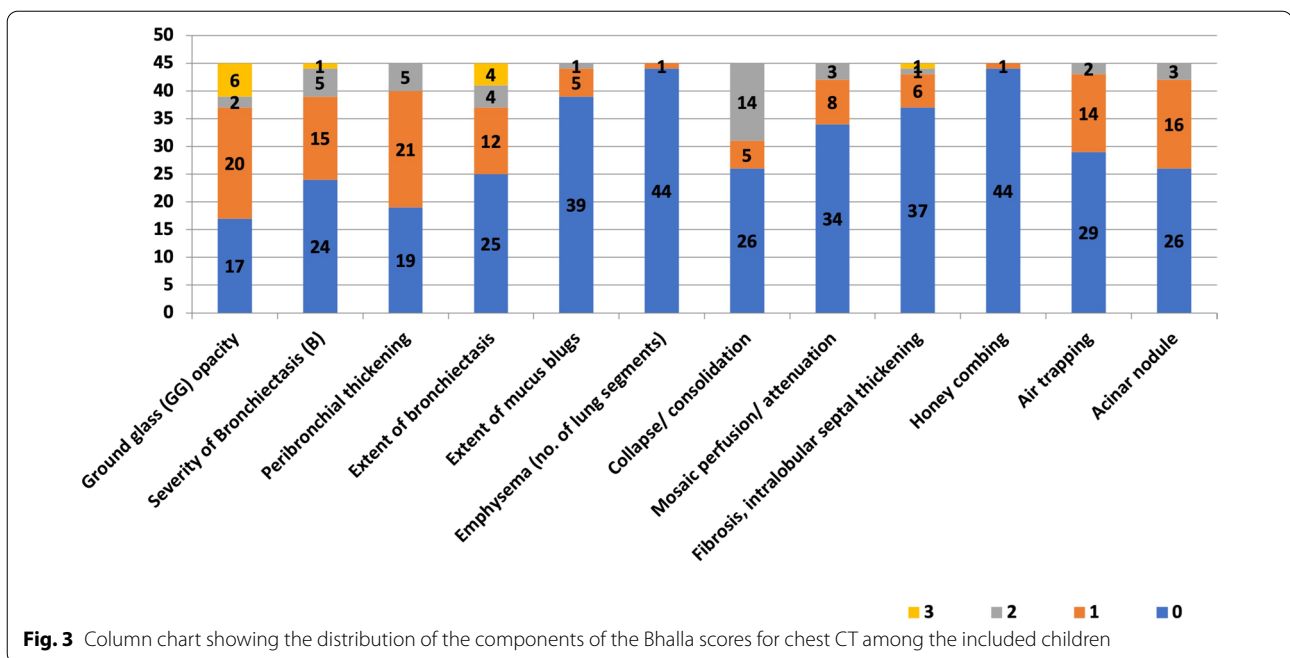


Fig. 3 Column chart showing the distribution of the components of the Bhalla scores for chest CT among the included children

Table 2 Various etiological diagnoses of studied cases with pediatric chronic lung disease

Chronic lung disease in pediatrics

Inhalation lung disease:

Hypersensitivity pneumonitis,
Toxin inhalation

Chronic recurrent inflammatory:

Recurrent viral/bacterial/fungal infection,
Granulomatous disease,
Aspiration

Autoimmune disease

Chronic airway disease:

Suppurative lung syndrome,
Asthma

ILD:

NEHI,
Pulmonary hemorrhage,
NSIP,
UIP,

Langerhans cell histiocytosis and edema

Hereditary malformations:

Congenital lobar emphysema,
CF,
Ciliary dyskinesia

Chronic vascular disease with recurrent infarction

ILD Interstitial lung disease; NEHI Neuroendocrine hyperplasia of infancy; NSIP Non-specific interstitial pneumonia; UIP Usual interstitial pneumonia; CF Cystic fibrosis

autoimmune disease, chronic airway disease, ILD, hereditary malformations, and vascular disease.

The Bhalla score, first proposed by Bhalla et al., was created to adjust for pulmonary structural damage observed on MDCT in pediatric cases diagnosed with CF in the year 1991 [6]. Thereafter, Judge et al. proposed modifications to the score by including more CT features described in the disease, namely mosaic attenuation/perfusion, air trapping, acinar nodule, intralobular septal thickening, and ground-glass infiltrate [8]. In the current study, the significance of CT scores in inflammatory and inhalation lung diseases suggests the utility of this scoring system for such entities as well.

The American Thoracic Society classified Childhood interstitial lung disease (chILD) by the age-group from infancy to later childhood presentation [10]. In the current study, 34 patients (75.6%) were diagnosed as chILD with mainly later childhood presentation, including inhalation, post-inflammatory, aspiration pneumonitis, autoimmune diseases, and ILD (including infants with NEHI and children with UIP, NSIP, and hemosiderosis). Clinical evaluation through further tests, such as high-resolution CT, spirometer tests, bronchoalveolar lavage, and biopsy, is needed [10].

Aspiration syndrome (Fig. 4) is a common finding in children with recurrent lower respiratory tract infections and is predicted to be present in 26–49% of children with chILD. One study showed consolidation or airway changes in the dependent and basal portions of both lungs on CT [11]. In the current study, aspiration

Table 3 Number of cases, total and mean CT scores for each etiological diagnosis

	Total number of cases	Total CT score	Mean CT score	P value
Inhalation	5	48	9.6	0.006*
Inflammatory	30	183	6.1	0.030*
Autoimmune	4	43	10.75	0.523
Hereditary	4	33	8.25	0.523
ILD	9	71	7.88	0.335
Chronic airway diseases	9	72	8	0.473
Vascular	3	12	4	0.508

ILD Interstitial lung disease, *Significant

syndrome was reported in 7 (11%) of the cases and 20.6% of chILD cases. Moreover, variable CT features had been observed among those with aspiration syndrome, which ranged from patchy ground-glass densities in 66.7%, bronchiectasis in 66.7%, and collapse in 33.3%. Moreover, those with aspiration syndrome had a disease located in the apical segment of both lower lobes (LL), with 50% showing diffuse LL involvement and 33.3% showing middle lobe and lingula involvement. Regarding disease incidence, a study by Deutsch et al. showed that only 1.7% of chILD cases were diagnosed with aspiration syndrome. However, the CT chest findings presented herein were consistent with those presented in a study conducted by Tanaka et al. wherein MDCT in 85 children diagnosed with aspiration syndrome revealed no significant correlation between aspiration syndrome and all CT features, except for bronchial wall thickening and atelectasis [12].

Neuroendocrine cell hyperplasia (NEHI) has been found to present more frequently among males in the first 2 years of life. MDCT, which has a sensitivity of 78% and specificity of 100% for NEHI, typically shows a mosaic attenuation pattern affecting at least four lobes with geographic ground-glass opacities that are most conspicuous on the right middle lobe and lingula and areas of hyperlucency associated with air trapping. Confirmatory biopsy may not be necessary for patients with a classic clinical presentation and characteristic radiologic findings [10]. The study by Deutsch et al. showed that NEHI was diagnosed in 10% of chILD cases [9]. These findings were consistent with our clinical and radiological data on confirmed NEHI cases, although they accounted for only 2.9% of our chILD cases (Fig. 5).

There are several causes of lung hemorrhage, including vasculitis, good pasture syndrome, and systemic lupus erythematosus. In the acute phase, CT findings show an ill-defined fluffy appearing centrilobular ground glass that represents diffuse alveolar hemorrhage. With repeated hemorrhage, mild interstitial fibrosis has been found to cause interlobular septal thickening [10]. In the current study, similar changes were noted in a single case

with repeated hemorrhage, who developed pulmonary alveolar hemosiderosis.

Langerhans cell histiocytosis is one of the chILD diseases that is not specific to infancy, with portions of the systemic disease with pulmonary involvement presenting in 20–50% of the cases [10]. CT shows nodules of varying size and bizarre pulmonary cyst shapes, with upper lobe predominance [13]. This was consistent with our case diagnosed with Langerhans cell histiocytosis (Fig. 6).

Our findings showed that ILD was significantly correlated with the presence of lung honeycombing ($P=0.044$), similar to the case with usual interstitial pneumonia (Fig. 7). This has been considered a common finding in fibrotic lung disease that leads to traction of bronchioles and formation of a honeycomb appearance. Studies have shown a significant correlation between ILD and honeycomb appearance on MDCT [14].

In the present study, 8.9% of the included cases presented with autoimmune disease, which was significantly correlated with bilateral lung affection and a higher number of emphysematous bullae. These findings were consistent with those presented in several studies including children diagnosed with systemic autoimmune disease, which found that autoimmune disease was significantly correlated with bilateral lung pathologies [15–17]. The presence of autoimmune lung disease had been commonly associated with pulmonary emphysema based on the available literature [18].

In the present cohort, the severity of lung disease and peribronchial thickening was significantly correlated with overall hereditary lung anomalies. These findings were consistent with those presented in studies conducted on children diagnosed with cystic fibrosis, which revealed that children with hereditary malformations of the bronchial tree and ciliary dyskinesia were predisposed to severe manifestations of bronchiectasis [19, 20].

In the current study, the three cases (6.7%) who had CF all presented with variable severity of bronchiectasis and peribronchial thickening, with two showing air trapping, one showing mucus plug formation, and another case

Table 4 Correlation of etiological diagnosis with CT chest components of Bhalla score

Spearman's correlation	Ground-glass opacity	Severity of bronchocentric tasis (B)	Peribronchial thickening	Extent of bronchiec-tasis	Extent of mucous plugs	Extent of sacculation	Abscesses or bronchial division involved	No. of bronchial bubbles	Emphy- Collapse/ consolidation	Mosaic perfusion/attenuation	Fibrosis, intralobular septal	Honey-combing	Air trapping	Acinar nodule	Total CT score		
Inhalation	Correlation	0.112	0.154	0.168	0.203	-0.138	0.09	0.166	-0.053	-0.294	0.337*	0.012	-0.053	0.019	0.418*	0.206	0.132
	P value	0.465	0.312	0.27	0.181	0.364	0.557	0.277	0.728	0.05	0.023*	0.936	0.728	0.899	0.004*	0.175	0.386
Inflammatory	Correlation	-0.253	-0.034	-0.072	-0.079	0.142	-0.053	-0.046	-0.213	0.381*	-0.392*	-0.420*	-0.213	0.054	-0.058	-0.178	-0.265
	P value	0.094	0.823	0.638	0.607	0.354	0.728	0.763	0.16	0.01	0.008*	0.004*	0.16	0.724	0.704	0.243	0.079
Autoimmune	Correlation	-0.003	0.177	0.139	0.237	0.133	0.127	0.156	0.483**	0.123	-0.008	0.05	-0.047	0.136	0.093	0.164	0.463**
	P value	0.983	0.245	0.362	0.116	0.385	0.407	0.305	0.001	0.421	0.958	0.746	0.759	0.372	0.544	0.282	0.001
Congenital	Correlation	-0.244	0.394*	0.358*	0.281	0.102	-0.11	0.239	-0.047	-0.154	0.036	-0.145	-0.047	0.136	-0.262	0.2	-0.097
	P value	0.107	0.007*	0.016*	0.062	0.505	0.471	0.113	0.759	0.314	0.814	0.343	0.759	0.372	0.082	0.187	0.524
ILD	Correlation	0.275	-0.031	0.014	0.019	-0.036	0.012	0.038	0.302*	-0.172	-0.043	0.650**	0.302*	-0.148	-0.007	0.155	0.225
	P value	0.067	0.84	0.926	0.901	0.813	0.939	0.805	0.044	0.257	0.78	0	0.044	0.332	0.962	0.308	0.137
Chronic airway disease	Correlation	-0.018	0.216	0.231	0.157	0.123	-0.176	0.241	-0.075	-0.172	0.108	-0.232	-0.075	0.332*	0.142	0.211	0.035
	P value	0.904	0.154	0.127	0.303	0.42	0.246	0.11	0.623	0.257	0.479	0.126	0.623	0.026	0.352	0.163	0.821
Vascular	Correlation	-0.311*	-0.091	-0.144	-0.229	-0.105	0.478**	-0.228	-0.04	-0.222	0.041	-0.124	-0.04	0.155	0.106	-0.131	-0.083
	P value	0.037	0.55	0.346	0.13	0.494	0.001**	0.133	0.793	0.143	0.788	0.418	0.793	0.308	0.488	0.389	0.586

* Correlation is significant at the P-value of 0.05 level, ** Correlation is highly significant at the P-value of 0.01 level

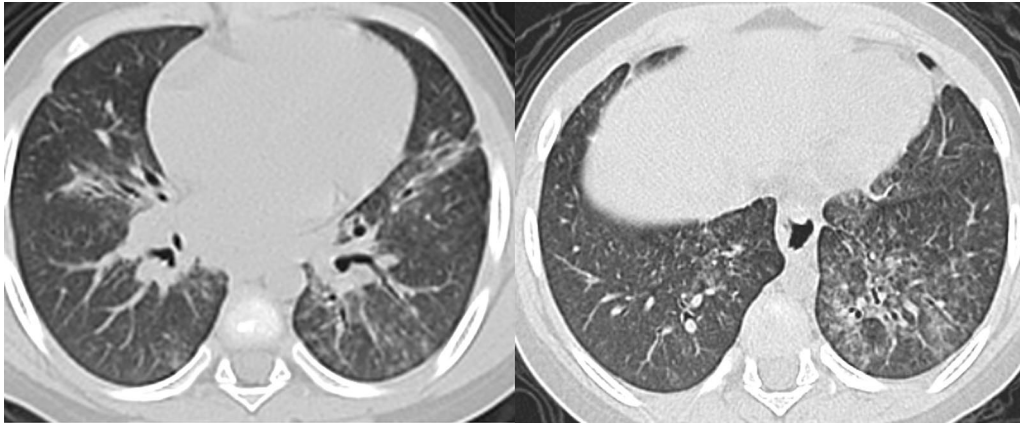


Fig. 4 A 5-year-old male with recurrent chest infection secondary to chronic aspiration showing bilateral bronchial wall thickening mainly in the lower lobes, centrilobular and peribronchial ground-glass densities, and hilar lymphadenopathy, with a CT score of 14

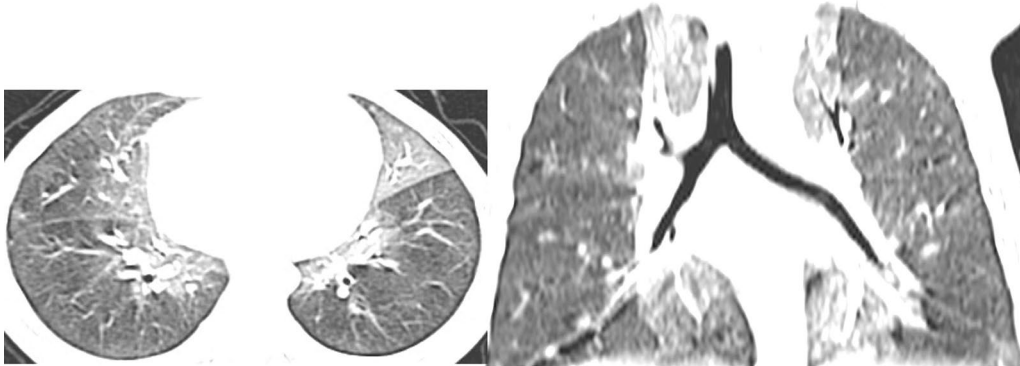


Fig. 5 A 1.5-year-old male with dyspnea and persistent oxygen requirement since birth, diagnosed with NEHI. Axial and coronal CT lung windows showed bilateral homogenous ground-glass densities mainly involving the medial lung fields with a well-defined lateral margin and a CT score of 5

showing collapse and ground-glass attenuation (Fig. 8). Sasihuseyinoglu et al. showed that out of 36 patients, 96.4% exhibited peribronchial thickening, 50 showed mucus plug formation, and 32.1% exhibited collapse/consolidation. Emphysema was identified in 18 patients [21].

The current study showed that the total CT score was significantly correlated with the severity and extent of bronchiectasis, along with peribronchial thickening. These findings were consistent with those presented in a multicenter prospective observational study by Martínez-García et al. in 99 consecutive patients with moderate-to-severe bronchiectasis, who showed that the severity of CLD was significantly correlated with the Bhalla CT score [22]. Similarly, another study on the Bhalla score showed an almost ninefold increase in the risk of having malacia/obliterative-like combination lesions in the bronchial tree [23].

Mosaic perfusion/attenuation and intralobular septal thickening was significantly correlated with the presence of inflammatory processes in lungs ($P=0.008$ and 0.004 , respectively). These findings were confirmed by Teufel and his team, who stated that mosaic attenuation was significantly correlated with the presence of lung inflammation [24]. However, this was inconsistent with another study conducted on patients with wet cough, which showed that inflammation was not significantly associated with the total Bhalla score [25].

The present study showed that chronic airway disease was associated with bronchial disease in 77.8%, mucous plugging in 22.2%, mosaic attenuation in 33.3%, and centrilobular nodules in 55.6% and was significantly correlated with air trapping ($P=0.026$) (Fig. 9). These findings were consistent with those presented in several studies conducted to evaluate the extent of expiratory air

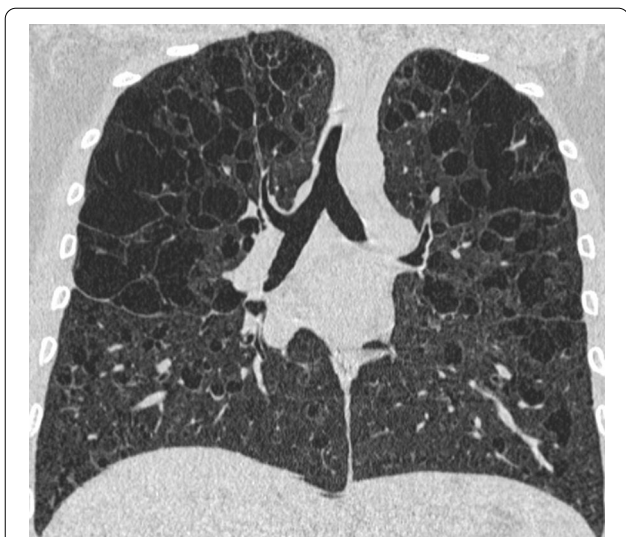


Fig. 6 A known case of Langerhans cell histiocytosis in a 16-year-old male with chronic progressive dyspnea showing bilateral, bizarrely shaped, thin wall cysts predominantly in the upper lobe and nodules; estimated CT score was 5

trapping on MDCT and spirometry, which concluded that air trapping was a prominent feature of chronic airway diseases, such as asthma and chronic bronchitis [26–28].

Thickening of the interlobular septa was found more frequently in cases with CLD mainly secondary to inflammatory and interstitial lung disease. One study showed that the prominent inflammatory infiltration into the submucosa of patients with idiopathic bronchiectasis might lead to lymphatic congestion and thus thickening of the interlobular septa [29].

The current study showed that 17.8% of cases exhibited respiratory distress, with a severity score ranging from 2 to 21, and that the clinical severity of symptoms was not correlated with the CT score. Douros et al. [23] stated that MDCT scanning detected airway wall thickening and bronchiectasis, with the severity of the findings correlating positively with the length of clinical symptoms. Moreover, they found that the clinical picture was incompatible with MDCT findings.

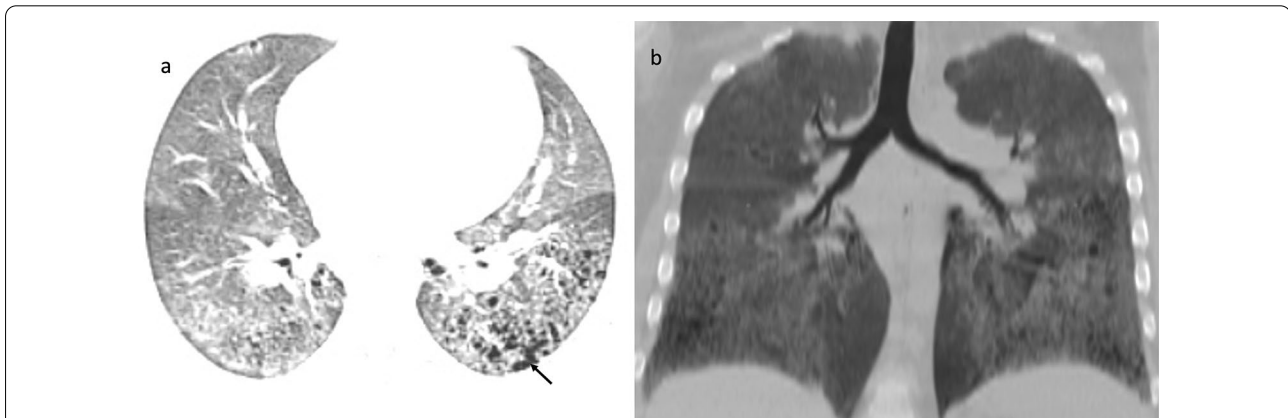


Fig. 7 A 10-year-old female diagnosed with usual interstitial pneumonia (IPF) complaining with progressive dyspnea, HRCT chest **a** axial cut and **b** minimum intensity projection (MinIP) showed bilateral fairly symmetric mainly lower lobes reticulations, with traction bronchiolectasis, bronchiolectasis and honeycombing (arrow), CT score 18

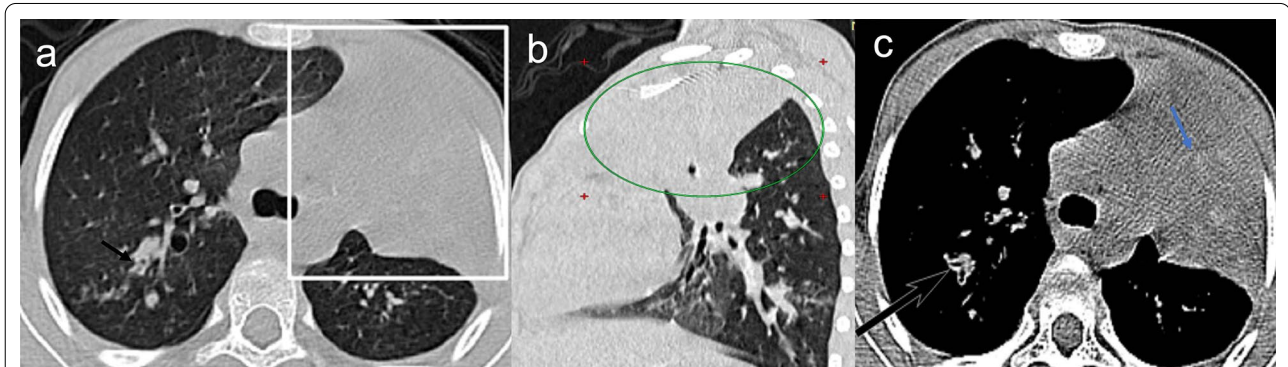


Fig. 8 Axial **(a)** and sagittal **(b)** reformatted chest CT images (lung window) showing total left upper lobar collapse, right posterior segment UL mild bronchiectasis, bronchial wall thickening, and bilateral ground-glass centrilobular nodules. Axial mediastinal window **(c)** showing left upper lobar dense internal contents of mucoceles (blue arrow), right posterior segment UL mild bronchiectasis and bronchial wall thickening (black arrows). A diagnosis of cystic fibrosis with secondary infection was established, estimated CT score was 11

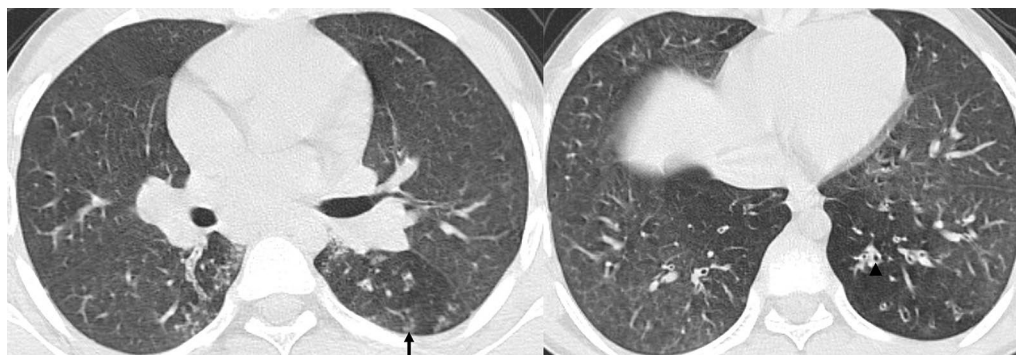


Fig. 9 A 11-year-old male, known tuberculous with a history of recurrent infection, CT chest mid and lower cuts showed bilateral bronchial wall thickening (arrowhead), left air trapping, centrilobular nodules (arrow), and tree in bud pattern, note fullness of both hila by lymph nodes, diagnosed as infectious bronchiolitis, estimated CT score was 14

It is important for clinicians and radiologists to work collaboratively in the radiological assessment of the rising number of children with CLD in order to provide continuous management and utilize the most optimal radiological procedures to ensure accurate clinical diagnosis and appropriate management pathways [2].

This study was limited by the limited number of cases which is hindered by the available cases over the study timing.

Conclusion

MDCT is a useful tool for diagnosing pediatric chronic lung disease (CLD) and assessing disease extent, severity, and superimposed complications. The modified Bhalla CT scoring system was allowed for primary and follow-up systematic radiological assessment of various lung lesions in cases with varying CLD etiologies and was not correlated with clinical severity.

Abbreviations

BPD: Bronchopulmonary dysplasia; CF: Cystic fibrosis; chILD: Childhood interstitial lung disease; CLD: Chronic lung disease; GERD: Gastroesophageal reflux disease; ILD: Interstitial lung disease; MDCT: Multidetector computed tomography; NEHI: Neuroendocrine hyperplasia of infancy; PFT: Pulmonary function test.

Acknowledgements

Not applicable.

Author contributions

ROM, CKM, and MAH reviewed the images. YSS, ROM, and CKS analyzed and interpreted the patient data. MAH wrote the manuscript and ROM, CKS, and YSS reviewed it. All authors have read and approved the manuscript.

Funding

The authors state that this work has not received any funding.

Availability of data and materials

The datasets used and/or analyzed during the current study are available from the corresponding author upon reasonable request.

Declarations

Ethics approval and consent for participate

Approval of the ethical committee of the 'Radiology department, Faculty of Medicine, Cairo University' was granted before conducting this prospective study; Reference number: not applicable. Local institutional review board approval was granted before conducting this cross-sectional study, and written informed consent was obtained from all patients.

Consent for publication

All patients included in this research gave written informed consent to publish the data contained within this study. If the patients were less than 16 years old, deceased, or unconscious when consent for publication was requested, written informed consent for the publication of these data was given by their parents or legal guardians.

Competing interests

The authors declare that they have no competing interests.

Author details

¹Diagnostic Radiology and Intervention, Kasr-Alainy Hospital, Cairo University Medical School, Cairo, Egypt. ²Paediatric Departments, Kasr-Alainy Hospital, Cairo University, Cairo, Egypt.

Received: 8 July 2022 Accepted: 17 December 2022

Published online: 27 December 2022

References

- Rossi SE, Franquet T, Volpacchio M, Gimenez A, Aguilar G (2005) Tree-in-bud pattern at thin-section CT of the lungs: radiologic-pathologic overview. *Radiographics* 25(3):789–801
- Rossi UG, Owens CM (2005) The radiology of chronic lung disease in children. *Arch Dis Child* 90(6):601–607
- Hoffman EA, Simon BA, McLennan G (2006) State of the art. A structural and functional assessment of the lung via multidetector-row computed tomography: phenotyping chronic obstructive pulmonary disease. *Proc Am Thorac Soc* 3(6):519–532
- Grenier PA, Beigelman-Aubry C, Fétiat C, Prêteux F, Brauner MW, Lenoir S (2002) New frontiers in CT imaging of airway disease. *Eur Radiol* 12(5):1022–1044
- Diab-Cáceres L, Girón-Moreno RM, García-Castillo E, Pastor-Sanz MT, Oliveira C, García-Clemente MM et al (2021) Predictive value of the modified Bhalla score for assessment of pulmonary exacerbations in adults with cystic fibrosis. *Eur Radiol* 31(1):112–120

6. Bhalla M, Turcios N, Aponte V et al (1991) Cystic fibrosis: scoring system with thin-section CT. *Radiology* 179:783–788
7. Helbich TH, Heinz-Peer G, Eichler I et al (1999) Cystic fibrosis: CT assessment of lung involvement in children and adults. *Radiology* 213:537–544
8. Judge EP, Dodd JD, Masterson JB, Gallagher CG (2006) Pulmonary abnormalities on high-resolution CT demonstrate more rapid decline than FEV1 in adults with cystic fibrosis. *Chest* 130(5):1424–1432. <https://doi.org/10.1378/chest.130.5.1424>
9. Deutsch GH, Young LR, Deterding RR et al (2007) Diffuse lung disease in young children, application of a novel classification scheme. *Am J Respir Crit Care Med* 176:1120–1128
10. Semple TR, Ashworth MT, Owens CM (2017) Interstitial lung disease in children made easier well almost. *Radiographics* 37(6):1679–1703
11. Zanetti G, Marchiori E, Gasparetto TD, Escuissato DL, Soares Souza A (2007) Lipoid pneumonia in children following aspiration of mineral oil used in the treatment of constipation: high-resolution CT findings in 17 patients. *Pediatr Radiol* 37(11):1135–1139
12. Tanaka N, Nohara K, Ueda A, Katayama T, Ushio M, Fujii N, Sakai T (2019) Effect of aspiration on the lungs in children: a comparison using chest computed tomography findings. *BMC Pediatr* 19(1):1–7
13. Sabri YY, Fouad MA, Assal HH, Abdullah HE (2016) Cystic lesions in multislice computed tomography of the chest: a diagnostic approach. *Egypt J Radiol Nucl Med* 47(4):1313–1322
14. Yamakawa H, Ogura T, Sato S, Nishizawa T, Kawabe R, Oba T et al (2020) The potential utility of anterior upper lobe honeycomb-like lesion in interstitial lung disease associated with connective tissue disease. *Respir Med* 172:106125
15. Levy DM, Kamphuis S (2012) Systemic lupus erythematosus in children and adolescents. *Pediatr Clin* 59(2):345–364
16. Das S, Langston C, Fan LL (2011) Interstitial lung disease in children. *Curr Opin Pediatr* 23(3):325–331
17. Vece TJ, Fan LL (2010) Interstitial lung disease in children older than 2 years. *Pediatr Allergy Immunol Pulmonol* 23(1):33–41
18. Staats P, Kligerman S, Todd N, Tavora F, Xu L, Burke A (2015) A comparative study of honeycombing on high resolution computed tomography with histologic lung remodeling in explants with usual interstitial pneumonia. *Pathol Res Pract* 211(1):55–61
19. Karadag B, Karakoc F, Ersu R, Kut A, Bakac S, Dagli E (2005) Non-cystic-fibrosis bronchiectasis in children: a persisting problem in developing countries. *Respiration* 72:233–238
20. Banjar HH (2007) Clinical profile of Saudi children with bronchiectasis. *Indian J Pediatr* 74:149–152
21. Sasihuseyinoglu AS, Altıntaş DU, Soyupak S, Dogruel D, Yılmaz M, Serbes M, Duyuler G (2019) Evaluation of high resolution computed tomography findings of cystic fibrosis. *Korean J Intern Med* 34(2):335
22. Martínez-García MA, de la Rosa Carrillo D, Soler-Cataluña JJ, Donat-Sanz Y, Serra PC, Lerma MA, Valdecillos MB (2013) Prognostic value of bronchiectasis in patients with moderate-to-severe chronic obstructive pulmonary disease. *Am J Respir Crit Care Med* 187(8):823–831
23. Douros K, Alexopoulou E, Nicopoulou A, Anthracopoulos MB, Fretzayas A, Yiallourous P et al (2011) Bronchoscopic and high-resolution CT scan findings in children with chronic wet cough. *Chest* 140(2):317–323
24. Teufel M, Ketelsen D, Fleischer S, Martirosian P, Graebler-Mainka U, Stern M et al (2013) Comparison between high-resolution CT and MRI using a very short echo time in patients with cystic fibrosis with extra focus on mosaic attenuation. *Respiration* 86(4):302–311
25. Chang AB, Boyce NC, Masters IB, Torzillo PJ, Masel JP (2002) Bronchoscopic findings in children with non-cystic fibrosis chronic suppurative lung disease. *Thorax* 57(11):935–938
26. Jain K, Padley SPG, Goldstraw EJ, Kidd SJ, Hogg C, Biggart E, Bush A (2007) Primary ciliary dyskinesia in the paediatric population: range and severity of radiological findings in a cohort of patients receiving tertiary care. *Clin Radiol* 62(10):986–993
27. Busacker A, Newell JD Jr, Keefe T, Hoffman EA, Granroth JC, Castro M et al (2009) A multivariate analysis of risk factors for the air-trapping asthmatic phenotype as measured by quantitative CT analysis. *Chest* 135(1):48–56
28. Schroeder JD, McKenzie AS, Zach JA, Wilson CG, Curran-Everett D, Stinson DS et al (2013) Relationships between airflow obstruction and quantitative CT measurements of emphysema, air trapping, and airways in subjects with and without chronic obstructive pulmonary disease. *Am J Roentgenol* 201(3):W460–W470
29. Ketai LH, Mohammed TL, Kirsch J et al (2014) ACR appropriateness criteria(R) hemoptysis. *J Thorac Imaging* 29(3):W19–22

Publisher's Note

Springer Nature remains neutral with regard to jurisdictional claims in published maps and institutional affiliations.

Submit your manuscript to a SpringerOpen® journal and benefit from:

- Convenient online submission
- Rigorous peer review
- Open access: articles freely available online
- High visibility within the field
- Retaining the copyright to your article

Submit your next manuscript at ► [springeropen.com](https://www.springeropen.com)
